Wind and Structures, *Vol. 29, No. 5 (2019) 323-337*
DOI: https://doi.org/10.12989/was.2019.29.5.323

Optimal wind-induced load combinations for structural design of tall buildings

C.M. Chan*[1], F. Ding[1], K.T. Tse[1], M.F. Huang[2], K.M. Shum[3] and K.C.S. Kwok[4]

[1]Department of Civil and Environmental Engineering, The Hong Kong Univ. of Science and Technology, Hong Kong
[2]Institute of Structural Engineering, Zhejiang University, Hangzhou, P. R. China
[3]CLP Power Wind/Wave Tunnel Facility, The Hong Kong University of Science and Technology, Hong Kong
[4]School of Civil Engineering, The University of Sydney, NSW 2006, Australia

(Received July 24, 2018, Revised May 7, 2019, Accepted May 14, 2019)

Abstract. Wind tunnel testing technique has been established as a powerful experimental method for predicting wind-induced loads on high-rise buildings. Accurate assessment of the design wind load combinations for tall buildings on the basis of wind tunnel tests is an extremely important and complicated issue. The traditional design practice for determining wind load combinations relies partly on subjective judgments and lacks a systematic and reliable method of evaluating critical load cases. This paper presents a novel optimization-based framework for determining wind tunnel derived load cases for the structural design of wind sensitive tall buildings. The peak factor is used to predict the expected maximum resultant responses from the correlated three-dimensional wind loads measured at each wind angle. An optimized convex hull is further developed to serve as the design envelope in which the peak values of the resultant responses at any azimuth angle are enclosed to represent the critical wind load cases. Furthermore, the appropriate number of load cases used for design purposes can be predicted based on a set of Pareto solutions. One 30-story building example is used to illustrate the effectiveness and practical application of the proposed optimization-based technique for the evaluation of peak resultant wind-induced load cases.

Keywords: wind tunnel test; load combinations; optimization-based framework; design envelope; tall buildings

1. Introduction

The accurate assessment of wind-induced load effects plays a pivotal role in the structural design of high-rise buildings. The wind tunnel physical modeling technique has long been recognized as an accurate and comprehensive experimental method for estimating wind loads on tall buildings, especially those with irregular shapes. The high frequency base balance (HFBB) test, which requires only simple models cut out of rigid but light weight foam plastic (Tschanz and Davenport 1983), has become one of the most common wind tunnel testing techniques. The HFBB test is capable of simultaneously measuring the aerodynamic wind loads that generate building vibrations in two translational directions and one torsional direction. For tall buildings with significant coupled lateral and torsional responses, the estimation of the peak resultant load effects is an extremely important issue in the assessment of building performance under wind excitation.

The peak vectorial combination effects can be determined through simplified rules, including the square-root-of-the-sum-of-squares (SRSS) or the complete-quadratic-combination (CQC) method. Isyumov (1982) proposed an approach for estimating the peak resultant load effects caused by wind forces in the two sway directions and the wind-induced torque by using the SRSS rule with empirical joint action factors. The values of the joint action factors range from 0.7 to 1.0, depending on the relative magnitudes of the two load components. These results have been reflected in the current American and Canadian building codes and standards. Nonetheless, this method is only suitable for buildings or structures with regular shapes and does not account for building specific aerodynamic effects.

Solari and Pagnini (1999) provided an analytical evaluation scheme of the vectorial load effects from alongwind and crosswind responses. A dodecagon representing the envelope of the critical load conditions was constructed, in which an elliptical threshold, defined by the maximum and minimum values of a single process, was enclosed. However, the correlation between the alongwind and crosswind load components was neglected, and the torsional load effect was not included in the establishment of the combined wind load cases for buildings with irregular structural configurations. For slender and flexible buildings, the AIJ Recommendations (2004) assume that the crosswind and torsional forces follow bivariate normal distributions in which the correlation between these two load components are taken into account. The equivalence line of probability can then be interpreted as an elliptical curve. An octagon enclosing the elliptical curve serves as an envelope to represent the critical load combinations along with a reduced value of the maximum alongwind force. In terms of the approaches for determining the value of the wind load combination factor, Tamura *et al*. (2008) proposed the combination factor for estimating the equivalent crosswind load along with the alongwind load

*Corresponding author, Professor
E-mail: cecmchan@ust.hk

http://www.techno-press.com/journals/was&subpage=7
ISSN: 1226-6116 (Print), 1598-6225 (Online)

that acted simultaneously on medium-rise buildings. Chen and Huang (2009) studied the upcrossing theory to evaluate the peak resultant response of wind-excited tall buildings from correlated three-dimensional responses. Naess *et al*. (2009) developed an efficient method for estimating extreme response statistics of the combined load effect processes, based on a Monte Carlo simulation. Bartoli et al. (2011) demonstrated a copula-based approach for evaluating the expected maxima of two or more linearly combined processes. Stathopoulos *et al.* (2013) presented load combination factors derived from wind tunnel tests for evaluating structural wind loads on rectangular medium-rise buildings. Kim *et al.* (2016) presented wind load combination rules based on the concept of combination factor using a simplified reference building with four columns for atypical supertall buildings. Huang *et al*. (2017) proposed a copula-based approach for determining dynamic wind load combinations for tall buildings.

Most previous studies have focused on the determination of the peak resultant load effects for a single process. Nonetheless, wind tunnel testing for measurement of the wind loads that act on a building should be carried out using various wind directions. Therefore, critical load cases, resulting from the time series in all wind directions, should be identified, and a limited number, accounting for governing conditions, may be selected for design. A general outline from the Boundary Layer Wind Tunnel Laboratory at the University of Western Ontario (2007) specifies that the nominal number of load cases covering all combinations of two translational moments and one torsional moment for all wind directions is 24. It is assumed that the largest load effects occur when the load in one principal load direction is at its peak together with nominal loads in the other two principal directions. Boggs and Lepage (2006) suggested 10 to 20 or so load cases, in which a critical load combination was either defined as the principal component experiencing its peak values with other two companion values, or the maximum vector resultant values.

Nonetheless, as far as the authors are aware, most if not all of the common practices for obtaining critical wind load cases, and the appropriate number of load cases, relies in part on subjective engineering judgment. Furthermore, because there are no general rules for wind load combinations, the estimated extreme wind load effects can vary greatly in different combination schemes. It is also important to realize that the use of existing combination methods may result in inconsistent and subjective assessments of the critical wind load effects on buildings.

This paper presents a computer-based optimization approach to determine the peak resultant load cases of wind-excited tall buildings with three-dimensional correlated wind loads measured in wind tunnel tests. A multivariate normal distribution is assumed for random wind-induced structural load components in each incident wind direction. The equivalence surface of probability can then be interpreted as an ellipsoid, corresponding to a certain statistical threshold. An optimization-based framework is proposed in the search for a convex hull that serves as a design envelope. The individual combined load cases can be expressed in terms of the coordinates of the vertices of the optimized polyhedron. The Pareto front is also integrated in this new method to enable the prediction of the appropriate number of load cases. A 30-story building is used as an illustrative example to demonstrate this systematic combination scheme. The accuracy of the proposed method with the current combination approach is evaluated, and a more precise estimation of wind load cases of tall buildings is achieved.

2. Commonly used practices for wind load combinations

2.1 Analysis of wind-induced response and equivalent static wind loads in HFBB tests

High frequency base balance (HFBB) testing has emerged during the past three decades as a powerful tool for determining the dynamic responses of tall buildings subjected to wind loads (Tschanz and Davenport 1983, Boggs and Peterka 1989). In HFBB tests, the time-variant base moment components in two translational directions and one twisting direction are simultaneously measured and are considered to be the aerodynamic loads that act on the building. For an *n*-story building modeled as a three-degrees-of-freedom system with a lumped mass at each floor level, the structural responses can be derived from the equation of motion, which is conveniently written in matrix notation as (Clough 1993)

$$[M]\{\ddot{x}\}+[C]\{\dot{x}\}+[K]\{x\}=\{F\} \tag{1}$$

where $[M]$, $[C]$, $[K]$, $\{x\}$ and $\{F\}$ are the mass matrix, matrix of damping coefficient, stiffness matrix, displacements and external forces, respectively. Since Eq. (1) represents a set of coupled differential equations to be solved, eigenvalue analysis is conducted, in which the coupled system can be conveniently transformed into a set of uncoupled equations as

$$m_j\ddot{\xi}_j+c_j\dot{\xi}_j+k_j\xi_j=f_j \tag{2}$$

where m_j, c_j, k_j, and f_j are the generalized mass, generalized damping, generalized stiffness and the generalized force for the *j*th mode as

$$\begin{aligned} m_j &= \{\phi_j\}^T[M]\{\phi_j\} \\ k_j &= \{\phi_j\}^T[K]\{\phi_j\} \\ c_j &= 2m_j\omega_j\zeta_j \\ f_j &= \{\phi_j\}^T\{F\} \end{aligned} \tag{3}$$

ξ_j is the generalized coordinate that can be expressed as

$$\xi_j=\{\phi_j\}^T\{x\} \tag{4}$$

ϕ_j is the *j*th mode shape vector. Since the base moments are measured in HFBB tests, the key issue is to link the external force or the generalized force to the base moments.

Assuming that the structure has a linear mode shape in the two swaying directions and a constant mode shape in the torsion direction (Boggs and Peterka 1989), the generalized force can be expressed by the base moments as

$$\begin{aligned} f_j &= \{\phi_j\}^T \{F\} \\ &= \sum[\eta_{xj}\phi_{xj}(z_i)F_x(z_i)+\eta_{yj}\phi_{yj}(z_i)F_y(z_i)+\eta_{\theta j}\phi_{\theta j}(z_i)F_\theta(z_i)] \\ &= \sum[\eta_{xj}\phi_{xj}(z_h)\frac{z}{h}F_x(z_i)+\eta_{yj}\phi_{yj}(z_h)\frac{z}{h}F_y(z_i)+\eta_{\theta j}\phi_{\theta j}(z_h)F_\theta(z_i)] \\ &= \frac{\eta_{xj}\phi_{xj}(z_h)}{h}M_y-\frac{\eta_{yj}\phi_{yj}(z_h)}{h}M_x+\eta_{\theta j}\phi_{\theta j}(z_h)M_\theta \end{aligned} \tag{5}$$

in which $\phi_j(z_h)$ is the value of jth mode shape vector at the top of the building; η_j is the mode shape correction factor; and M_x, M_y, M_θ are measured time series of the base moments from HFBB tests.

Using the HFFB technique, simultaneous base shears, moments and torques are measured at the base of an aerodynamic building model in a boundary-layer wind tunnel, after which the response of the building may be calculated for any combination of the building's mass, stiffness, damping and the oncoming wind speed. As the aerodynamic wind force is a random function, the base moment response spectrum of the building can be calculated by random vibration theory in the frequency domain as (Zhou *et al.* 2003)

$$S_M(f)=|H(f)|^2 S_m(f) \tag{6}$$

where S_M is the base moment response spectrum; S_m is the input aerodynamic wind load spectrum; H is the mechanical admittance function which can be computed as

$$|H(f)|^2=\frac{1}{\left[1-(f/f_o)^2\right]^2+4\zeta^2(f/f_o)^2} \tag{7}$$

where f_o is the modal frequency of the building and ζ is the critical damping ratio.

The mean square response moment can be calculated by integrating the area underneath the moment response spectrum curve given in Eq. (6) as

$$\sigma_M^2=\int_0^\infty S_M(f)df=\int_0^\infty |H(f)|^2 S_m(f)df \tag{8}$$

In general, the mean square response can be approximated as the sum of background component and resonant component as follows (Davenport 1995)

$$\sigma_M^2=\sigma_{MB}^2+\sigma_{MR}^2 \tag{9}$$

The background component of the mean square base m oment response can be considered as quasi-static and is given as

$$\sigma_{MB}^2=\int_0^\infty S_m(f)df \tag{10}$$

For a lightly damped system, the resonant component of the mean square moment response can be simplified by the white noise assumption and obtained approximat ely as

$$\sigma_{MR}^2 \approx S_m(f_o)\int_0^\infty |H(f)|^2 df=\frac{\pi}{4\zeta}f_o S_m(f_o) \tag{11}$$

Using the gust response factor approach and dividin g the peak response in terms of mean, background and resonant components, the peak base moment can be re written as (Kareem and Zhou 2003)

$$\hat{M}=\overline{M}+\sqrt{\hat{M}_B^2+\hat{M}_R^2} \tag{12}$$

where the background component $\hat{M}_B$ and the resona nt component $\hat{M}_R$ could be estimated from Eqs. (8) and (9) respectively as

$$\hat{M}_B=g_B\sigma_{MB} \tag{13}$$

$$\hat{M}_R=g_R\sigma_{MR}=g_R\sqrt{\frac{\pi}{4\zeta}f_o S_m(f_o)} \tag{14}$$

in which the background peak factor, g_B, can be approximated by the peak factor of the oncoming wind velocity, the value of which is usually assumed to be about 3 to 4 (Zhou *et al.* 1999). For a Gaussian process, the resonant peak factor, g_R, can be given as (Davenport 1967)

$$g_R=\sqrt{2\ln f_0\cdot T}+\frac{0.577}{\sqrt{2\ln f_0\cdot T}} \tag{15}$$

where T is the observation time (usually 3600 s).

By means of the HFFB technique, the time history of the base moments is first measured, the power spectral density of the base moments $S_m(f)$ is then derived. With the derived $S_m(f)$ spectrum curve, the RMS values of such base moments are then computed using Eq. (8) and the expected peak base moments are calculated by Eq. (12). Based on the calculated peak base moments, the wind-induced structural loads (or the so-called ESWLs) on the building can then be given by distributing the peak base moment to the floor levels over the building height (Homes 2002, Chen and Kareem 2004). Similar to the base moments, the ESWLs expressed in terms of total peak floor load, $\hat{F}$, can also be written into a linear combination of the mean ($\overline{F}$), the background ($W_B\hat{F}_B$) and the resonant ($W_R\hat{F}_R$) responses as

$$\hat{F}=\overline{F}+W_B\hat{F}_B+W_R\hat{F}_R \tag{16}$$

where $W_B=\frac{\sigma_{MB}}{(\sigma_{MB}^2+\sigma_{MR}^2)^{1/2}}$, $W_R=\frac{\sigma_{MR}}{(\sigma_{MB}^2+\sigma_{MR}^2)^{1/2}}$; $\hat{F}_B$ is the peak background wind loads and $\hat{F}_R$ is the peak resonant wind loads.

Using Eq. (16), the ESWLs can be expressed respectively in the alongwind, crosswind and torsional directions of a building. For convenience of discussion, the

X- and Y-axes denote the alongwind and crosswind directions, respectively, and the vertical Z-axis defines the torsional direction of the building. In theory, the mean component of both the crosswind and torsional wind loads should be equal to zero. The alongwind mean force can be related to the approaching wind velocity profile and written as follows

$$\bar{F}_x(z) = \frac{1}{2}\rho\bar{U}_H^2\left(\frac{z}{H}\right)^{2\alpha} BC_D \tag{17}$$

where ρ=the air density; $\bar{U}_H$ =the wind speed at the top of the building; α=the power law exponent; B=the width of the building; *CD* = the drag force coefficient of the building.

Due to the quasi-static nature of the background component of the wind loads, the distribution of which can be assumed to follow the distribution of the mean alongwind loading profile given in Eq. (17) as (Zhou *et al*. 1999)

$$\hat{F}_{Bx,y}(z) = \frac{\bar{F}(z)}{\int_0^H \bar{F}(z)zdz}\hat{M}_{Bx,y} \tag{18a}$$

$$\hat{F}_{B\theta}(z) = \frac{\bar{F}(z)z}{\int_0^H \bar{F}(z)zdz}\hat{M}_{B\theta} \tag{18b}$$

where $\hat{F}_{B_{x,y,\theta}}(z)$ is the peak background wind load, and $\bar{F}(z)$ is the mean alongwind load.

For a building having uncoupled mode shapes defined as $\phi_x(z), \phi_y(z), \phi_\theta(z)$, the distribution of the resonant component of the generalized wind loads follows basically the inertial load distribution as shown in Eq. (19(a)) for the translational X- or Y- direction and Eq. (19(b)) for the rotational direction.

$$\hat{F}_{R_{x,y}}(z) = \frac{m(z)\phi_{x,y}(z)}{\int_0^H m(z)\phi_{x,y}(z)zdz}\hat{M}_{R_{x,y}} \tag{19a}$$

$$\hat{F}_{R\theta}(z) = \frac{I(z)\phi_\theta(z)}{\int_0^H I(z)\phi_\theta(z)dz}\hat{M}_{R_\theta} \tag{19b}$$

where $\hat{F}_{R_{x,y,\theta}}(z)$ is the peak resonant wind load along the height, *m(z)* is the mass per unit height, *I(z)* is the rotational mass moment of inertia about the vertical axis through the center of mass per unit height. For a more general building with complex three dimensional mode shapes, the ESWLs can be similarly evaluated with due consideration of the lateral-torsional mechanical coupling effects as well as the intermodal coupling of modal responses (Chan *et al*. 2010).

2.2 Determination of design wind load cases in one wind direction

Once the equivalent static wind loads have been derived, as described in Section 2.1, they can further be used to estimate the extreme wind load cases. The expected extreme values of alongwind and crosswind moment responses can be represented in a two-dimensional manner by an elliptical threshold. As shown in Fig. 1, the coordinates of the elliptical center are given as the mean values of the two base moment response components, and the magnitudes of the major and minor axes of the ellipse are interpreted as the maximum fluctuating parts of two response components, respectively, which are equal to the product of the standard deviations and the peak factor. By further considering the correlation between two wind load components by Boggs (2014), an inclined ellipse as shown in Fig. 2 presents the extreme wind load conditions. Its skewness indicates the correlation coefficient of two wind load components.

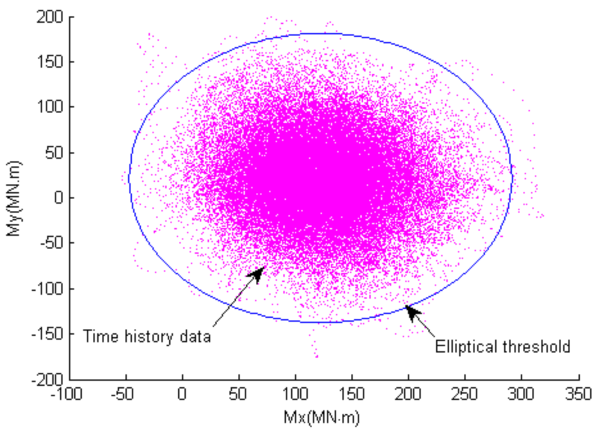

Fig. 1 Elliptical threshold without consideration of wind load correlation

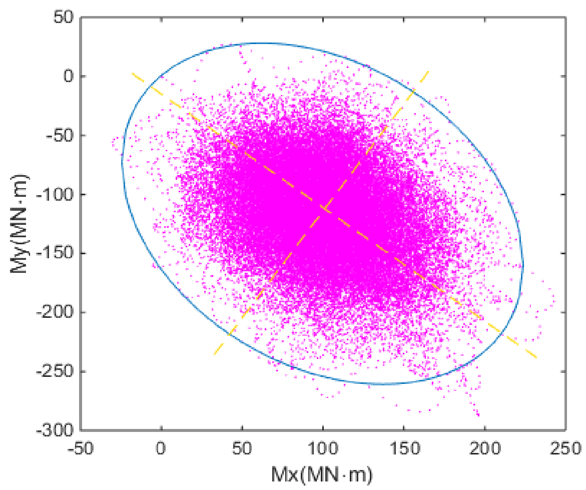

Fig. 2 Elliptical threshold with consideration of wind load correlation

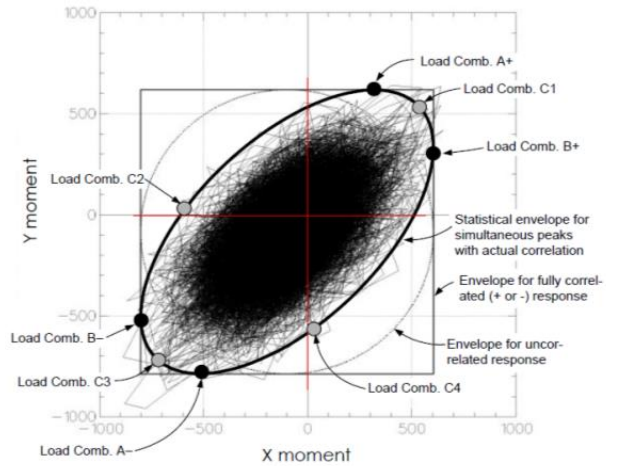

Fig. 3 Inner approximation of the elliptical threshold (Boggs 2014)

After an elliptical threshold is developed, extreme wind load cases should be identified subsequently. The design wind loads are required to be presented in the form of equivalent static loads with a limited number for consideration (Xie *et al*. 1999). In theory, every point on the threshold can be regarded as a probable extreme wind load combination; but it is not practical to consider all of them. Instead, to interpret the limited number of the wind load cases, the approximation rule should be proposed, which can be generally categorized into the inner and outer approximation for the elliptical threshold. In the context of the inner approximation, two principles are established for the selection of the critical load combinations: one is called principal-companion loads (Type A and B in Fig. 3), and another is called the maximum vector resultant (Type C in Fig. 3) (Boggs 2014). Those load combinations can be considered as the vertices of the inner polygon of the ellipse.

2.3 Consideration of wind directionality

With respect to the wind directional effects, all elliptical thresholds corresponding to each incident wind direction measured in HFBB test should be considered, which dramatically increases the difficulty to select the critical load cases from all the ellipses.

To overcome this difficulty, one approach is to directly use the wind load combinations located on the integrated elliptical threshold expressed by the heavy line in Fig. 4 as the design wind load cases. In theory, every point on the integrated envelope in Fig. 4 can be regarded as a statistically-derived extreme wind load combination; but it is not easily to mathematically define the integrated threshold enveloping all ellipses. Furthermore, it is neither necessary nor practical to consider all of the possible points on the integrated envelope.

Another approach is to construct a polygon which serves as a design envelope of all elliptical thresholds in Fig. 5. Each wind load case is interpreted as a vertex on the polygon, and can be determined by best preserving the shape of the integrated elliptical boundary with some increases of the reliability level due to outer approximation. Those vertexes are the representatives of the principle wind load component with the positive or negative companion load component, or the maximum resultant load effects. This paper aims at developing an automated and more accurate approach in defining the extreme wind load combinations using the polygonal design envelope in 2-dimensional manner and the polyhedral design envelope in 3 dimensions.

3. Two-dimensional optimization framework for development of design envelope

3.1 Development of elliptical threshold for two load components

For each incident wind direction, an elliptical threshold is first developed in which the correlation obtained from the statistical analyses of the time series between each two base moment responses is taken into account.

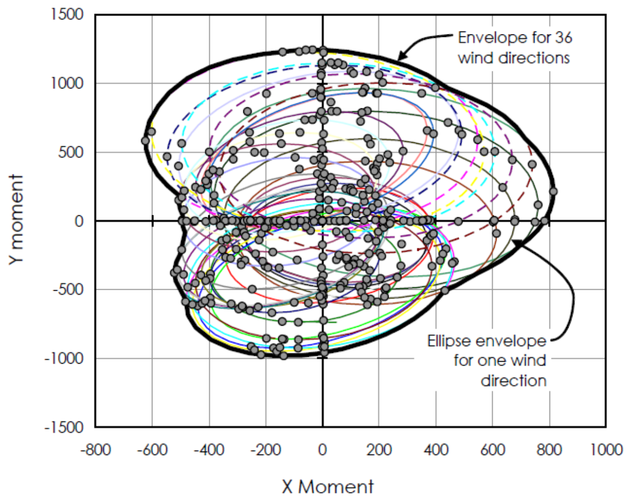

Fig. 4 Wind load combinations considering wind directionality (Boggs 2014)

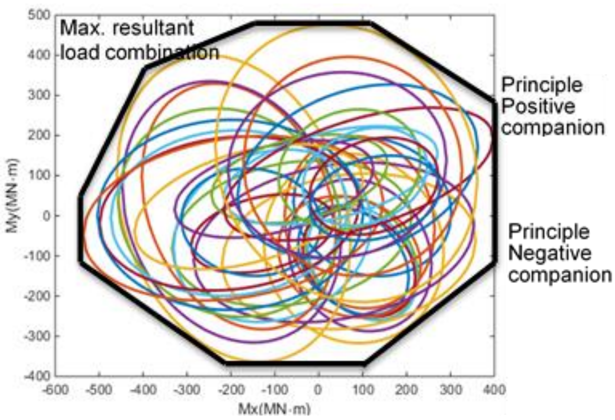

Fig. 5 Polygonal envelope for elliptical thresholds

It is assumed that the two base moment responses follow a bivariate normal distribution, as proposed in the AIJ Recommendations (Tamura *et al.* 2003a), and the joint probability density function (PDF) is written as (Lin 1976)

$$p(M_i^{norm}, M_j^{norm}) = \frac{1}{2\pi\sqrt{1-\rho^2}} \times \exp\left[-\frac{\left(M_i^{norm}\right)^2 - 2\rho M_i^{norm} M_j^{norm} + \left(M_j^{norm}\right)^2}{2(1-\rho^2)}\right]; \quad (i, j = x, y, \theta;\ i \neq j) \tag{20}$$

where ρ is the correlation coefficient of the base moment responses M_i and M_j; M_i^{norm} and M_j^{norm} are the two normalized base moment responses, given by

$$M_i^{norm} = \frac{M_i - \bar{M}_i}{\sigma_{M_i}}, M_j^{norm} = \frac{M_j - \bar{M}_j}{\sigma_{M_j}} \tag{21}$$

where $\bar{M}_i$, $\bar{M}_j$ and σ_{M_i}, σ_{M_j} are the mean values and standard deviations of the base moment responses. Concerning the correlation coefficient, the distribution forms an elliptical isopleth with a sloped major axis, as shown in Fig. 2. The magnitudes of the major and minor axes of the elliptical threshold denoted as a and b are expressed as (Kasperski 1992)

$$a = \sqrt{2(1+\rho)\left[\ln\left(\frac{1}{2\pi\sqrt{1-\rho^2}}\right) - \ln p(M_i^{norm}, M_j^{norm})\right]} \tag{22}$$

$$b = \sqrt{2(1-\rho)\left[\ln\left(\frac{1}{2\pi\sqrt{1-\rho^2}}\right) - \ln p(M_i^{norm}, M_j^{norm})\right]} \tag{23}$$

The statistical maxima of one specific response in a no rmalized form is defined by

$$\hat{M}_i^{norm} = \frac{\hat{M}_i - \bar{M}_i}{\sigma_{M_i}} = g \tag{24}$$

in which g is the peak response factor. The coordinate of another response component along with the specific maximum response becomes (Kasperski 1992)

$$\tilde{M}_j^{norm} = g\rho \tag{25}$$

The cumulative density function (CDF) that represents the confidence level of the elliptical threshold can be expressed as

$$\begin{aligned} &P(M_i^{norm}, M_j^{norm}) \\ &= \iint p(M_i^{norm}, M_j^{norm}) dM_i^{norm} dM_j^{norm} \\ &= \iint \frac{1}{2\pi\sqrt{1-\rho^2}} \times \\ &\exp\left[-\frac{(M_i^{norm})^2 - 2\rho M_i^{norm} M_j^{norm} + (M_j^{norm})^2}{2(1-\rho^2)}\right] dM_i^{norm} dM_j^{norm} \end{aligned} \tag{26}$$

To obtain the explicit formula of the CDF in terms of the peak factor, the Cartesian coordinates are transformed into polar coordinates (Fenn 2001). By further substituting Eq. (24) and Eq. (25) into Eq. (26) and evaluating the integral from minus infinite to the two normalized base moments, the probability of the two normalized base moment response corresponding to a particular level of confidence reflected by an associated peak factor g can be written as

$$P(M_i^{norm}, M_j^{norm}) = 1 - \exp(-0.5g^2) \tag{27}$$

The exceedance probability based on the assumption of Gaussian processes for two base moment responses becomes

$$P_E = 1 - P(M_i^{norm}, M_j^{norm}) = \exp(-0.5g^2) \tag{28}$$

The elliptical threshold is thus considered a statistical boundary that depicts the extreme wind load combinations in terms of the specified value of the peak factor. The ellipses corresponding to all incident wind directions are then integrated to form the closed statistical boundary of the two base moment responses, which represents all of the critical wind loads based on the entire set of test data, as shown in Fig. 7.

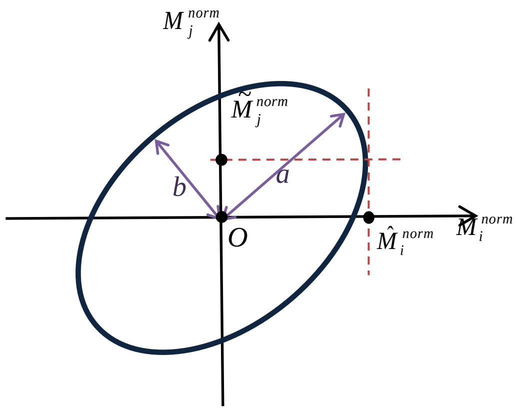

Fig. 6 Elliptical isopleth of two base moment response s in a normalized form

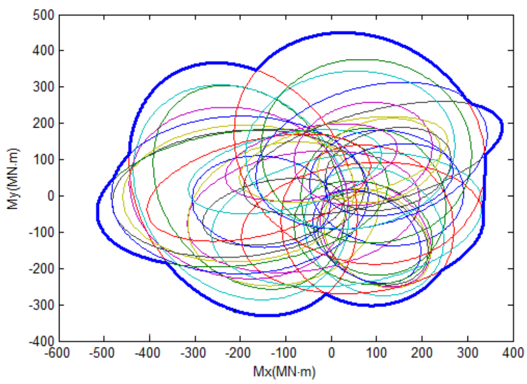

Fig. 7 Integrated elliptical threshold of two base moment response components for all incident wind directions

When developing the base moment ellipses corresponding to different wind directions, we have incorporated the appropriate transformations to convert the climate data to the reference wind speed used in the wind tunnel study. Given with the meteorological data of the local wind climate, different design wind speeds can be adjusted for different wind directions corresponding to an equal probability of occurring can be established. Using a probability approach, the desired value of base moment ellipse for each wind direction can be computed via the up-crossings method (Isyumov *et al.* 2014).

3.2 Optimization framework for obtaining 2D design envelope

In this section, a method will be developed for selection of a finite number of discrete critical load cases representing the integrated design wind load envelope. In search for the optimal design envelope that encompasses the critical wind load cases as its vertices, one major goal of this study is to develop a numerical optimization technique for the definition of a polygonal envelope that encloses the integrated elliptical thresholds while attaining as far as possible the minimum deviation.

3.2.1 Design variables

The formulation of this optimization problem starts with the determination of the design variables that are varied during the optimization process. For polygonal approximation with n vertices, the design variables are defined as the coordinates of each vertex $((x_1, y_1), (x_2, y_2), \ldots, (x_n, y_n))$ in $\mathbb{R}^2$.

3.2.2 Objective functions

In this proposed optimization framework for obtaining the polygonal threshold as a representative of the design envelope, the objective function is delineated by minimizing the area of the polygonal envelope. The reason is that the polygon with the smallest area in an outer approximation indicates that the difference between the polygonal and the integrated elliptical thresholds has been reduced to a minimum in terms of the shape distortion. The optimized polygonal envelope can thus be considered to be a practical representation of the statistically-derived elliptical thresholds and the overestimation of the critical wind load combinations is minimized.

A simple means of numerical calculation of the area of a convex polygon is to split the polygon into several triangles and calculate the sum of their areas. Each line segment of the polygon can be chosen as a base, and any inner point of the polygon can be chosen as an apex. Supposing that the line segment k connects two adjacent vertices (x_k, y_k) and (x_{k+1}, y_{k+1}) and that (x_o, y_o) denotes any inner point of the polygon, the formula for the area above can be written as half of a 3×3 determinant (Fenn 2001)

$$S_{\Delta_{o-k}} = \frac{1}{2}\begin{vmatrix} x_o & y_o & 1 \\ x_k & y_k & 1 \\ x_{k+1} & y_{k+1} & 1 \end{vmatrix} \tag{29}$$

By calculating the sum of the areas of all of the collective triangles, the total area of the polygon with n lines is given as

$$S_{polygon} = \sum_n S_{\Delta_{o-k}} \ (k = 1, 2, \ldots, n) \tag{30}$$

The objective function of the optimization problem can thus be defined as minimizing the value of $S_{polygon}$ through optimization of the coordinates of each vertex of the polygon by

$$Minimize \quad S_{polygon} = \sum_n S_{\Delta_{o-k}} \tag{31}$$

3.2.3 Constraint functions

Constraints are defined as restrictions that must be satisfied to ensure the feasibility of a design requirement. They are associated with certain physical phenomena in the optimization problem. In this framework, a polygonal approximation is undertaken to obtain the design envelope, in which the design problem involves constraints to guarantee that the estimated load cases remain at a certain confidence level while being representative of all peak resultant load effects. The variable bounds are also required to set the feasible region of each design variable.

Constraints for outer approximation

The outer approximation of the polygon based on the elliptical thresholds is used in this optimization framework to avoid underestimating the peak resultant loads and ensure a certain confidence level. The elliptical thresholds $\mathcal{E}_s$ for the wind direction s need to be contained in the polygonal subset denoted as $\mathcal{C}$. Mathematically, such a restriction can be given implicitly for an HFBB test under s = 1, 2,…,d number of incident wind directions as follows

$$\mathcal{E}_s = \left\{(x, y) \middle| x^2 - 2\rho_s xy + y^2 = g^2(1-\rho_s^2)\right\} \subseteq \mathcal{C} \quad (s = 1, 2, \ldots, d) \tag{32}$$

where ρ_s is the correlation coefficient for the selected two base moment responses for the wind direction s. To explicitly express Eq. (32), linear mapping is conducted so that each elliptical threshold can be transformed to a unit circle S^1 by

$$\varphi_s\colon\ \mathcal{E}_s \longrightarrow S^1 \qquad \mathcal{C} \longrightarrow \mathcal{C}' \tag{33}$$

where φ_s can be obtained from eigenvalue analysis of the covariance matrix of the normalized base moment r esponses by

$$\left[Cov(M_i^{norm}, M_j^{norm})\right]_s \phi_s = \phi_s \boldsymbol{D} \quad (i, j = x, y, \theta; i \neq j) \tag{34}$$

in which $\boldsymbol{D}$ is the unit diagonal matrix. After linear mapping, each elliptical threshold is eventually transformed into a unit circle centered at the origin. It is known that the circle S^1 is enveloped by the polygon $\mathcal{C}'$ when all points on the lines of the polygon are outside a circle in which the distance from the center of the circle should not be less than its radius. The general equation of a line of the polygon $\mathcal{C}$ through two adjacent vertices (x_k, y_k) and (x_{k+1}, y_{k+1}) can be written in a compact form as (Fenn 2001)

$$A_k \cdot X = b_k \tag{35}$$

where X=(x,y) and A=(a_1,a_2) are non-zero. A and b can be expressed in terms of the vertex coordinates, which are treated as design variables in the optimization problem as

$$A_k = \left(\frac{y_{k+1} - y_k}{x_k - x_{k+1}}, 1 \right); \quad b_k = \frac{x_k y_{k+1} - x_{k+1} y_k}{x_k - x_{k+1}} \tag{36}$$

To ensure an outer approximation of the design polygon that encloses the transformed circular threshold, the distance from the origin to each line segment of the polygon after linear mapping φ_s cannot be less than the radius equal to 1 as

$$\text{distance} = \left(\frac{|b_k^{'}|}{|A_k^{'}|} \right)_s \geq 1 \quad (k = 1, 2, ..., n;\ s = 1, 2, ..., d) \tag{37}$$

Constraints for convexity

Because not all the vertices on the concave polygon are representative of extreme wind load conditions, the second type of constraint keeps the polygonal design envelope convex so that every vertex, as one critical load combination, can be selected for practical use. A polygon $\mathcal{C}$ is said to be convex if, for any two points in $\mathcal{C}$, the line segment joining the two points is contained in $\mathcal{C}$ (Audin 2003). One simple means to ensure that a convex polygonal load envelope is generated is to make all vertices of the polygon lie on one side of any line segment of two consecutive vertices of the polygon. As shown in Fig. 9, for any pair of two adjacent vertices denoted as f and h on $\mathcal{C}$, $\mathcal{C}$ is a convex polygon if all of the other vertices are found to lie in a half-plane of the line segment joining f and h in compliance with the following requirements

$$\left(A_k \cdot X_f - b_k\right)\left(A_k \cdot X_h - b_k\right) > 0\ ; \\ (k=1,2,...,n;\ f,h=1,2,...,n;\ f,h \notin line\, k) \tag{38}$$

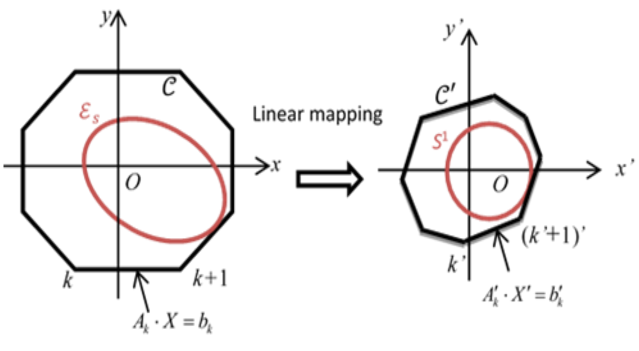

Fig. 8 Linear mapping for outer approximation

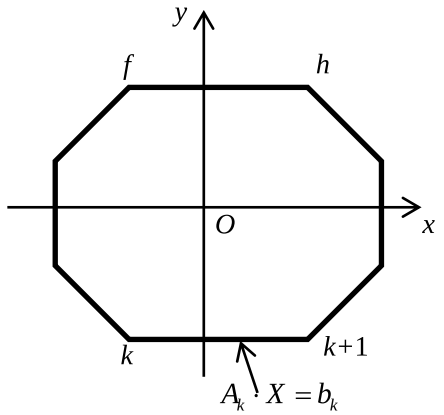

Fig. 9 Restrictions for convexity of the polygon

Side constraints

To avoid undue conservatism in the determination of a critical load case, the coordinates of each vertex of the polygonal design envelope must be limited within the statistical minimum and maximum values determined by

$$M_{i,\max} = M_i \pm g\sigma_{M_i} \qquad (i = x, y, \theta) \tag{39}$$

Therefore, the upper and lower bounds for the normalized base moment responses at the vertex of k are defined as

$$-g \leq x_{ki} \leq g \qquad (k = 1, 2, ..., n; i = x, y, \theta) \tag{40}$$

3.2.4 Optimization algorithms

The minimization of the area of the convex polygonal design envelope with n vertices enclosing the elliptical thresholds corresponding to the number of d incident wind directions can be summarized as follows

$$\text{Minimize} \quad S_{polygon} = \sum_n S_{\Delta_{o-k}} \ (k = 1, 2, ..., n) \tag{41a}$$

Subject to:

$$\left(\frac{|b_k^{'}|}{|A_k^{'}|} \right)_s \geq 1\ ; \qquad (k = 1, 2, ..., n;\ s = 1, 2, ..., d) \\ \left(A_k \cdot X_f - b_k\right)\left(A_k \cdot X_h - b_k\right) > 0; \\ (k=1,2,...,n;\ f,h=1,2,...,n;\ f,h \notin line\, k) \\ -g \leq x_{ki} \leq g\ ; \qquad (k=1,2,...,n;\ i=x,y,\theta) \tag{41b}$$

Once the optimization problem is formulated with the objective function and the design constraints explicitly expressed in terms of vertex coordinates as design variables, the optimization solution can then be sought by the sequential quadratic programming (SQP) method.

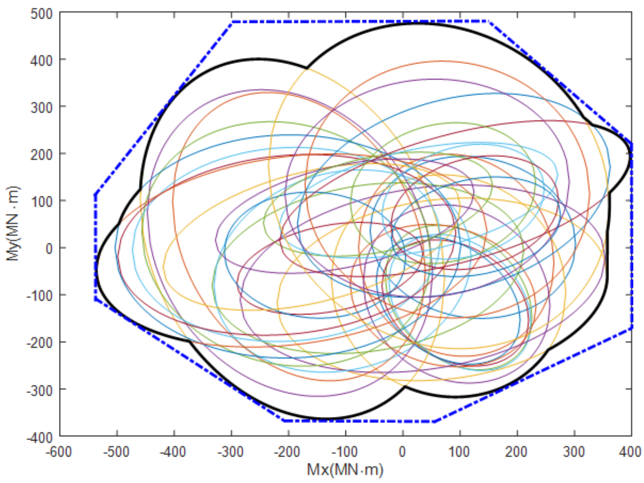

Fig. 10 Optimal polygonal design envelope for 2-dimensional wind load combinations

The SQP method starts with an initial design X^0, and a new and improved design point is then obtained as $X^1=X^0+\alpha^0X^0$ based on the properly chosen move limits. The optimal search direction is given in terms of the Hessian matrix of the Lagrangian function which is updated by the BFGS formula in the optimization process (Belegundu and Chandrupatla 2011). The gradient vectors are evaluated at the new design point and the above sequential process for formulation and solution of approximate QP problems is repeated until the minimum area of the convex polygon is attained while satisfying all of the specified design constraints.

This optimization framework is applied to obtaining wind load combinations regarding two load components. In the proposed framework, subjective judgment can be successfully avoided with the aid of this automated optimization technique. All the critical wind load conditions are more accurately presented through the optimal design envelope that best preserve the shape of the elliptical thresholds. Fig. 10 shows an eight-sided octagonal design envelope that best superscribes all elliptical thresholds with the least area of the octagonal envelope.

4. Three-dimensional optimization framework for development of the design envelope

4.1 Development of the ellipsoidal threshold for three load components

In Section 3, an optimization framework is proposed for the determination of wind load combinations in two dimensions. Indeed, wind loads that simultaneously act on tall buildings typically contain three load components: two lateral and one torsional. Because each load component does not reach its peak value at the same instant as the others, it is more significant to consider simultaneously the three-dimensional wind load combinations for structural design.

To obtain the peak resultant load effects for each incident wind direction, the ellipsoidal threshold is constructed at the beginning in a manner similar to the development of the elliptical threshold described in Section 3.1. The multivariate normal distribution is assumed for two translational and one torsional base moment responses by

$$p(X)=\frac{1}{(2\pi)^{1.5}|\Sigma|^{1/2}}\exp(-\frac{1}{2}X^T\Sigma^{-1}X) \tag{41}$$

where X and Σ denote variables for the normalized base moment responses and their covariance matrix, respectively, as

$$X=[M_x^{norm}\ M_y^{norm}\ M_\theta^{norm}];\Sigma=\begin{bmatrix}1 & \rho_{xy} & \rho_{x\theta}\\ \rho_{xy} & 1 & \rho_{y\theta}\\ \rho_{x\theta} & \rho_{y\theta} & 1\end{bmatrix} \tag{42}$$

Given the correlation coefficient, the multivariate normal distribution in Eq. (41) forms an ellipsoidal contour surface with a tilted major axis. The extreme wind load combinations for the three-dimensional base moment responses are then depicted as the ellipsoidal threshold. The lengths of the semi-principal axes are correlated with the value of the peak factor g. To explicitly express the relationship between the above two factors, a linear mapping from the general ellipsoid to a standard one centered at the origin and aligned with the axes is conducted by

$$\varphi':\ \varepsilon_{general}\rightarrow\varepsilon_{standard} \tag{43}$$

where φ' can be obtained from eigenvalue analysis of the covariance matrix of the normalized base moment responses by

$$[Cov(X)]\phi'=\phi'[Cov(X')] \tag{44}$$

in which the covariance matrix for the transformed variables $X'=[M_x^{norm'}\ M_y^{norm'}\ M_\theta^{norm'}]$ is diagonal. The equation for the standard ellipsoid then becomes

$$\frac{\left(M_x^{norm'}\right)^2}{\sigma^2_{x^{norm'}}}+\frac{\left(M_y^{norm'}\right)^2}{\sigma^2_{y^{norm'}}}+\frac{\left(M_\theta^{norm'}\right)^2}{\sigma^2_{\theta^{norm'}}}=g^2 \tag{45}$$

The CDF that represents the confidence level of the ellipsoidal threshold can be expressed as

$$P(X')=\iint\frac{1}{2\pi\sigma_{x^{norm'}}\sigma_{y^{norm'}}\sigma_{\theta^{norm'}}}\times\exp\left\{-\frac{1}{2}\left[\frac{(M_x^{norm'})^2}{\sigma^2_{x^{norm'}}}+\frac{(M_y^{norm'})^2}{\sigma^2_{y^{norm'}}}+\frac{(M_\theta^{norm'})^2}{\sigma^2_{\theta^{norm'}}}\right]\right\}dM_x^{norm'}dM_y^{norm'}dM_\theta^{norm'} \tag{46}$$

To obtain the explicit formula of the CDF in terms of the peak factor, the Cartesian coordinates are transformed into polar coordinates and the CDF can be rewritten as a function of the peak factor g as

$$P(X)=P(X')=2\Phi(g)-1-\frac{\sqrt{2}g}{\sqrt{\pi}}e^{-\frac{g^2}{2}} \tag{47}$$

where Φ is the cumulative probability for the standard normal distribution.

4.2 Optimization framework for obtaining three-dimensional design envelope

Once the ellipsoidal thresholds that correspond to wind approaching from all azimuths are established, an envelope enclosing all ellipsoidal thresholds can be developed for design purposes. A specified number of discrete critical load cases is determined by searching for the optimal design envelope interpreting critical wind load cases as its vertices. In this section, a numerical optimization technique is extended in three dimensions for direct definition of a convex polyhedron that encloses the ellipsoidal thresholds that correspond to all incident wind directions while providing the best fit to the original statistical boundary developed in Section 4.1.

4.2.1 Design variables

Consider a polyhedron with m triangular surfaces and n vertices; the design variables are defined as the coordinates of each vertex $((x_1, y_1, z_1), (x_2, y_2, z_2), \ldots, (x_n, y_n, z_n))$ in $\mathbb{R}^3$.

4.2.2 Objective functions

For three-dimensional wind load combinations, the objective function is delineated as minimizing the volume of the polyhedral envelope. A simple method of numerical calculation of the volume of a convex polyhedron with an irregular shape is to split it into several tetrahedrons and calculate the sum of their volumes. Each triangular face can be chosen as a base, and any inner point of the polyhedron can be chosen as an apex. Suppose three adjacent points (x_k, y_k, z_k), $(x_{k+1}, y_{k+1}, z_{k+1})$ and $(x_{k+2}, y_{k+2}, z_{k+2})$ interpret one surface k of the polyhedron and (x_o, y_o, z_o) denotes the inner point, the volume of the tetrahedron O-k is (Fenn 2001)

$$V_{o-k}=\frac{1}{6}\begin{vmatrix} x_k-x_o & y_k-y_o & z_k-z_o \\ x_{k+1}-x_o & y_{k+1}-y_o & z_{k+1}-z_o \\ x_{k+2}-x_o & y_{k+2}-y_o & z_{k+2}-z_o \end{vmatrix} \tag{48}$$

By adding together the volumes of all of the collective tetrahedrons, the total volume of the polyhedron with m surfaces can be determined, and the objective function can thus be defined as minimizing the value of the total volume through optimization of the coordinates of each vertex of the polyhedron by

$$Minimize \quad V_{polyhedron}=\sum_{k=1}^{m}V_{o-k} \tag{49}$$

4.2.3 Constraint functions

In this optimization framework, constraint functions are used to ensure that the approximated polyhedron encloses all of the ellipsoidal thresholds determined by the time series of 3D ESWLs while retaining the convexity of the polyhedron.

<u>*Constraints for outer approximation*</u>

Similar to the two-dimensional case, the outer approximation is used to avoid underestimating the peak resultant loads. This type of constraint is defined so that each ellipsoidal threshold $\mathcal{E}_s$ corresponding to wind direction s is contained in the polyhedral subset denoted as $\mathcal{C}$. After the linear mapping by Eq. (43), the restriction can be given implicitly for s=1,2,…,d incident wind directions, as follows

$$\mathcal{E}'_s=\left\{(x',y',z')\left|\frac{x'^2}{\sigma^2_{x^{norm'}}}+\frac{y'^2}{\sigma^2_{y^{norm'}}}+\frac{z'^2}{\sigma^2_{\theta^{norm'}}}=g^2\right)\right\}\subseteq\mathcal{C}' \tag{50}$$

$$(s=1,2,\ldots,d)$$

To explicitly express the above constraint function, each standard ellipsoidal threshold is further transformed to a unit sphere S^2 centered at the origin by

$$\varphi''_s:\ \mathcal{E}'_s\longrightarrow S^2\ \ \mathcal{C}'\longrightarrow\mathcal{C}'' \tag{51}$$

It is known that the sphere S^2 is enveloped by the polyhedron $\mathcal{C}''$ when the distance from the center of the sphere to each surface of the polyhedron is not less than its radius. The general equation of a surface k of the polyhedron $\mathcal{C}$ through three adjacent vertices (x_k, y_k, z_k), $(x_{k+1}, y_{k+1}, z_{k+1})$ and $(x_{k+2}, y_{k+2}, z_{k+2})$ can be written in compact form as (Fenn 2001)

$$A_k\cdot X=b_k \tag{52}$$

where $X=(x,y,z)$ and $A=(a_1,a_2,a_3)$ are non-zero. A and b can be expressed in terms of design variables as

$$A_k=\begin{bmatrix}(y_{k+1}-y_k)(z_{k+2}-z_k)-(y_{k+2}-y_k)(z_{k+1}-z_k)\\(z_{k+1}-z_k)(x_{k+2}-x_k)-(z_{k+2}-z_k)(x_{k+1}-x_k)\\(x_{k+1}-x_k)(y_{k+2}-y_k)-(x_{k+2}-x_k)(y_{k+1}-y_k)\end{bmatrix}^T; \tag{53}$$
$$b_k=A_k\cdot X_k{}^T$$

The constraint function for surface k of the polyhedron and the ellipsoidal threshold $\mathcal{E}_s$ can be written as

$$\text{distance}=\left(\frac{|b''_k|}{|A''_k|}\right)_s\geq 1\quad (k=1,2,\ldots,m;\ s=1,2,\ldots,d) \tag{54}$$

<u>*Constraints for convexity*</u>

This type of constraint keeps the polyhedral design envelope convex so that each vertex, as a representative of one critical load combination, can be selected for practical use. The polyhedron $\mathcal{C}$ is said to be convex if all of its vertices are located at the same side of each surface of the polyhedron. The constraint function is then defined that the sign convention should be kept the same for the function values of each vertex, and the function is checked with every two adjacent vertices. For instance, for any two vertices f and h on the polyhedron, the constraint function can be expressed as

$$\left(A_k \cdot X_f - b_k\right)\left(A_k \cdot X_h - b_k\right) > 0\ ; \quad (k = 1,2,...,m;\ f, h = 1,2,...,n;\ f, h \notin surface\, k) \tag{55}$$

Side constraints

The coordinates of each vertex v of the polyhedral design envelope serving as design variables must be limited within the statistical minimum and maximum values of normalized base moment responses by

$$-g \le x_{vi} \le g \qquad \left(v = 1,2,...,n;\ i = x, y, \theta\right) \tag{56}$$

4.2.4 Optimization algorithms

The minimization of the volume of the convex polyhedral design envelope with m triangular surfaces and n vertexes enclosing ellipsoidal thresholds corresponding to the number of d incident wind directions can be summarized as follows

$$\text{Minimize} \qquad V_{polyhedron} = \sum_{k=1}^{m} V_{o-k} \tag{57a}$$

Subject to:

$$\left(\frac{\left|b_k''\right|}{\left|A_k''\right|}\right)_s \ge 1 \quad (k = 1,2,...,m;\ s = 1,2,...,d)\ ;$$

$$\left(A_k \cdot X_f - b_k\right)\left(A_k \cdot X_h - b_k\right) > 0\ ; \quad (k = 1,2,...,m;\ f, h = 1,2,...,n;\ f, h \notin surface\, k) \tag{57b}$$

$$-g \le x_{vi} \le g \qquad \left(v = 1,2,...,n;\ i = x, y, \theta\right).$$

Once the optimization problem is formulated with the objective function and the design constraints are explicitly expressed in terms of the design variables, the nonlinear optimization solution can then be sought by SQP method.

This optimization framework is applied to systematically obtain the three-dimensional wind load combinations. Particularly, it will benefit the determination of the design wind load cases for tall buildings with complex structural configurations, for which three load components are equally important. Traditional methods are no longer deemed a feasible way to go since the critical loads are impossible to be determined simply by observations. Once the optimal design envelope is obtained with the specified number of load cases, the coordinates of each vertex will be representative of a critical wind load case for structural design. Results for a practical building are discussed in Section 5.

5. Illustrative examples

5.1 A 30-story building and the wind tunnel test

A study of a 30-story residential building was carried out to illustrate the effectiveness of this proposed optimization-based wind load combination approach. The floor plan of the building is shown in Fig. 11. A wind tunnel test was conducted at the CLP Power Wind/Wave Tunnel Facility (WWTF) of the Hong Kong University of Science and Technology. A 1:300 scale rigid model shown in Fig. 12 was subjected to approaching wind profiles of the 50-year return period for 36 attacking wind angles at 10° intervals for the 360° azimuth and was examined in the HFBB test to obtain the aerodynamic base moments of the structure.

Once the finite element model was set up for this building, an eigenvalue analysis was carried out to obtain the natural frequencies as well as the three-dimensional coupled mode shapes, as presented in Fig. 13. The first natural frequencies for three fundamental modes were 0.306 Hz, 0.368 Hz and 0.737 Hz, respectively. After determining the dynamic properties of the building, a dynamic analysis of the structure in the time domain was conducted to obtain the base moment responses in two translational directions and one torsional direction, corresponding to a duration of 3600 s.

The ellipsoidal threshold at each incident wind direction, based on the multivariate normal distribution, was derived from the time history samples. In terms of evaluating the peak fluctuating responses that affect the size of the ellipsoid, the background and resonant peaks are determined separately and then combined for total responses as

$$\hat{M} = \sqrt{(g_b \sigma_{M,b})^2 + (g_R \sigma_{M,R})^2} \tag{58}$$

The peak background factor g_b is typically taken as 3.5, and the peak resonant factor is calculated from the Davenport's formula as (Davenport, 1967)

$$g_R = \sqrt{2\ln f_i \tau} + 0.5772 / \sqrt{2\ln f_i \tau} \qquad (i = 1,2,3) \tag{59}$$

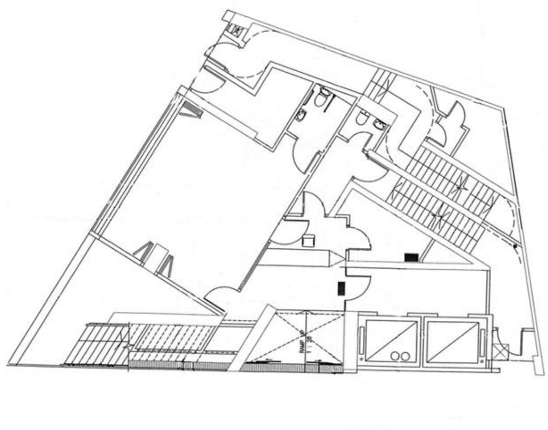

Fig. 11 Floor plan for a 30-story building

Fig. 12 The HFBB test for a 30-story building

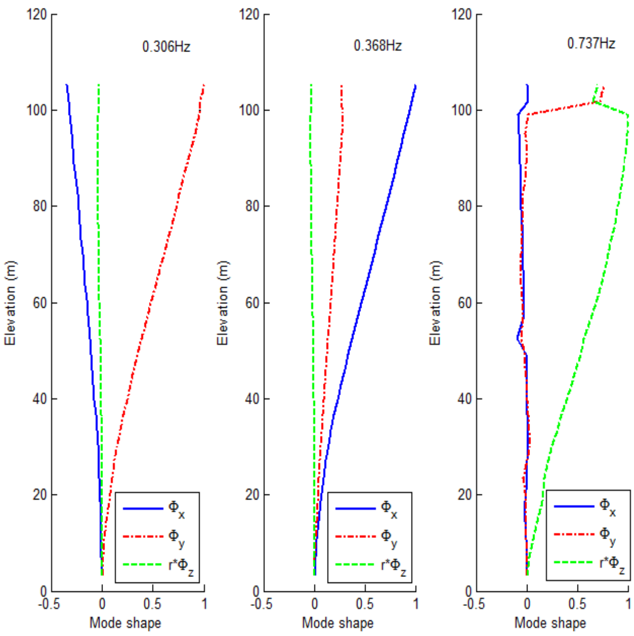

Fig. 13 Mode shapes of a 30-story building

where f_i stands for the frequency of the structure at mode i; τ represents the observation time duration that is generally 3600s. In this example, the first three modes are utilized for determination of peak resonant responses.

The proposed optimization-based framework was used to search for the minimum volume of the polyhedral design envelope with a given number of load cases that encloses the ellipsoidal thresholds corresponding to all wind directions. The Pareto front was then established to determine the appropriate number of wind load cases.

5.1 Results and discussion

Fig. 14 presents the ellipsoidal statistical boundary of the three-dimensional base moment responses at the incident wind direction of 300°. The dots represent the time history data of the base moment responses at 300°. The proposed three-dimensional optimization-based framework is then used to search for a convex polyhedral design envelope to contain all ellipsoidal thresholds while minimizing the shape distortion of the ellipsoidal thresholds.

The SQP method is used to systematically obtain the optimal design envelopes as an approximation of the probable extreme wind load combination interpreted as ellipsoidal thresholds, as shown in Fig. 15 for a range of 8 to 28 load cases. The coordinates of each vertex in the optimal design envelope are representative of a set of critical wind load cases.

Because the volume is considered to be an index for the examination of the departure of the approximated polyhedron from the original integrated statistical boundary, the least difference concerning the volumes implies that the approximated design envelope provides the best representation of the maximum combined wind load cases that are closest to the actual ones acting on the building. In general, the consideration of more load cases leads to a design envelope with a lesser volume. Therefore, the volumes for the increasing number of load cases of the design envelopes show a descending trend (Fig. 16), which indicates that the conservativeness for structural design is decreased. However, the magnitudes of the decreases in the volumes lead to convergence when the number of load cases is equal to 24. It should be recognized that a notable decrease in the volume corresponding to 24 load cases is captured because the design envelope with 24 vertices can be considered a better shape approximation, in which one prominent maximum or minimum load component along with the other two companion positive or negative load components are all taken into account.

For this building, the optimized design envelope with 24 wind load cases is recommended since this design envelope gives the smallest volume of the envelope.

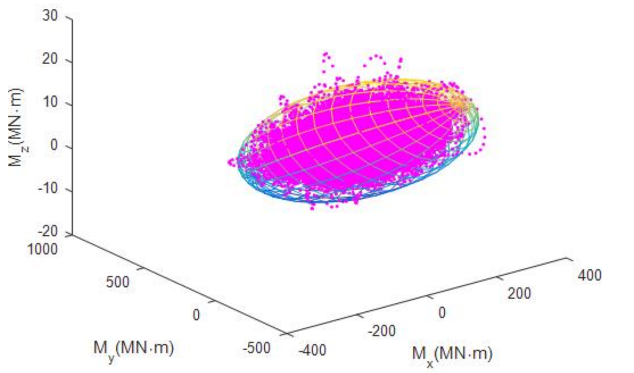

Fig. 14 Ellipsoidal threshold at the wind angle of 300°

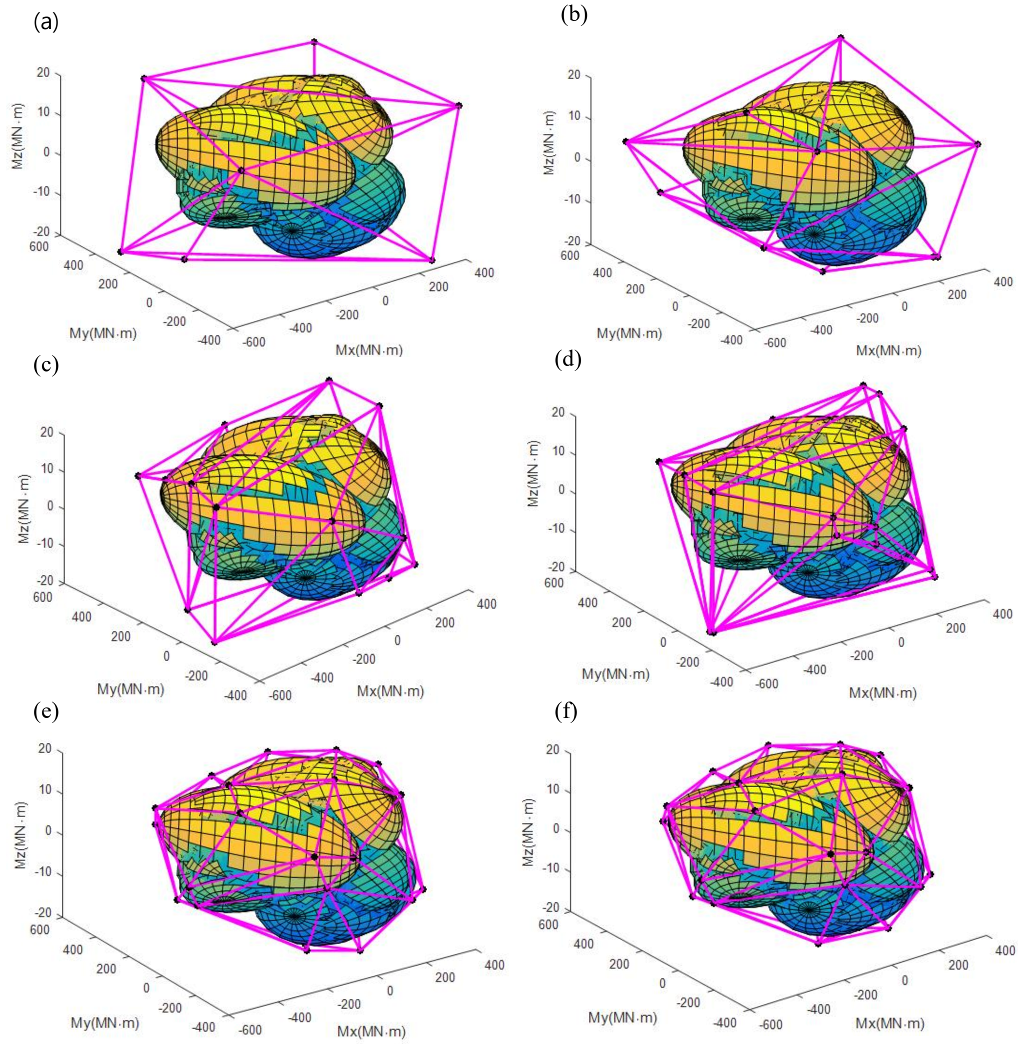

Fig. 15 Optimized design envelopes: (a) With 8 wind load cases, (b) With 12 wind load cases, (c) With 16 wind load cases, (d) With 20 wind load cases, (e) With 24 wind load cases and (f) With 28 wind load cases

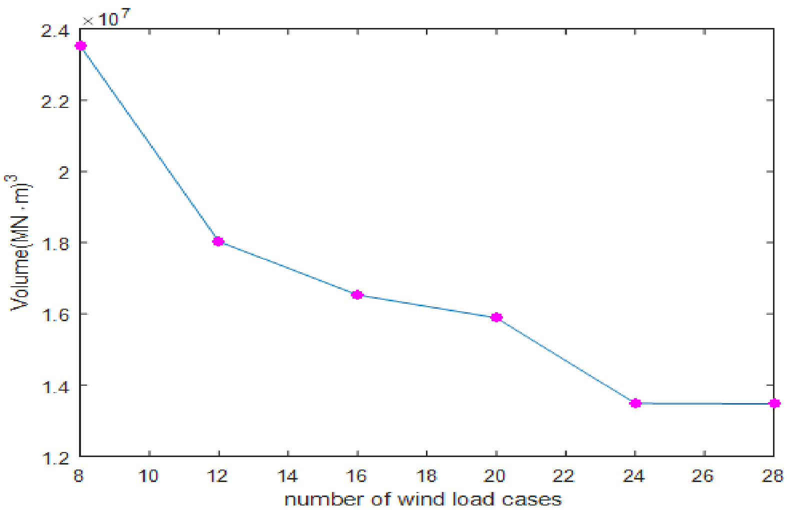

Fig. 16 The Pareto front for volumes of envelopes

Table 1 24 design wind load cases determined by the optimization-based approaches

Number	Design wind load cases		
	M_x(MN•m)	M_y(MN•m)	M_z(MN•m)
1	77.4	-26.8	17.7
2	230.7	187.3	17.3
3	-242.4	129.8	17.7
4	-343.5	-86.9	17.7
5	304.8	-92.4	11.7
6	397.4	185.2	11.1
7	147.9	476.0	11.2
8	-79.4	476.1	9.1
9	-434.8	286.9	11.3
10	-536.4	-62.2	2.1
11	-227.9	-363.7	11.6
12	-69.1	-363.7	9.0
13	397.3	-85.6	-12.8
14	397.4	287.0	7.8
15	82.1	476.1	-2.1
16	-358.3	401.1	3.4
17	-536.4	3.6	-2.5
18	-536.3	-117.8	-1.2
19	-176.7	-363.7	3.2
20	206.1	-307.1	-7.2
21	53.8	-219.9	-19.1
22	202.2	28.6	-19.1
23	-67.9	-66.9	-19.1
24	-142.4	-187.5	-16.7

A further increase in the number of wind cases from 24 to 28 does not appear to reduce the volume of the design envelope. It is evident that this optimization-based framework is capable of determining a set of peak resultant wind load cases as well as its number while achieving the accurate prediction of the critical wind loads by best representing the shape of the ellipsoidal thresholds with the aid of the optimization technique.

6. Conclusions

This study addressed the development of a combination scheme for obtaining the critical load cases of tall buildings on the basis of wind tunnel tests. Once the statistical boundary for the base moment responses is derived, an optimization framework is proposed for the systematic determination of the design wind load cases. Because there are as yet no universal rules to stipulate the number of wind load cases needed for design, an equilibrium analysis of the Pareto optima is also applied to discover a possibly equitable number of wind load cases. Results on a 30-story residential building have shown that this optimization technique provides a powerful tool for the assessment of extreme wind load effects. Not only is this technique capable of the systematic determination of critical wind load combinations without any subjective judgment, it also provides more accurate prediction of wind load cases while maintaining the conservativeness derived from statistical analysis.

Acknowledgments

The work described in this paper was partially supported by the Research Grants Council of the Hong Kong Special Administrative Region, China (Project No. 16200714), and was based upon research conducted by F. Ding under the supervision of C.M. Chan and K.T. Tse for the degree of Master of Philosophy in Civil Engineering at the Hong Kong University of Science and Technology. Thanks also go to the staff of the CLP Power Wind/Wave Tunnel Facility at the Hong Kong University of Science and Technology for their assistance in this project.

References

ASCE 7-05 (2005), *Minimum Design Loads for Buildings and Other Structures*, ASCE.

Audin, M. (2003), *Geometry*, Berlin: Springer.

Bartoli, G., Mannini, C. and Massai, T. (2011), "Quasi-static combination of wind loads: A copula-based approach", *J. Wind Eng. Ind. Aerod.*, **99**(6-7), 672-681. https://doi.org/10.1016/j.jweia.2011.01.022.

Belegundu, A. and Chandrupatla, T. (2011), *Optimization Concepts and Applications in Engineering*, New York: Cambridge University Press.

Boggs, D. (2014), "The past, present and future of high-frequency balance testing", *Wind Struct.*, **18**(4), 323-345. https://doi.org/10.12989/was.2014.18.4.323.

Boggs, D. and Lepage, A. (2006), "Wind tunnel methods", (Ed. Bracci, J.M.), *Performance-Based Design of Concrete Buildings for Wind Loads*, Special publication SP-240, American Concrete Institute, Michigan, 125-142.

Boggs, D. and Peterka, J. (1989), "Aerodynamic model tests of tall buildings", *J. Eng. Mech.*, **115**, 618-635. https://doi.org/10.1061/(ASCE)0733-9399(1989)115:3(618).

Chan, C.M., Huang, M.F. and Kwok, K.C.S. (2010), "Integrated wind load analysis and stiffness optimization of tall buildings with 3D modes", *Eng. Struct.*, **32**(5), 1252-1261. https://doi.org/10.1016/j.engstruct.2010.01.001.

Chen, X. and Huang, G. (2009), "Evaluation of peak resultant response for wind-excited tall buildings", *Eng. Struct.*, **31**, 858-868. https://doi.org/10.1016/j.engstruct.2008.11.021.

Chen, X. and Kareem, A. (2004), "Equivalent static wind loads on tall buildings: New model", *J. Struct. Eng. - ASCE,* **130**(10), 1425-1435.

Clough, R. and Penzien, J. (1993), *Dynamics of Structures*, McGraw-Hill, New York.

Davenport, A.G. (1967), "Gust loading factors", *J. Struct. Div.*, **93**(3), 11-34.

Davenport, A.G. (1995). "How can we simplify and generalize wind loading?", *J. Wind Eng. Ind. Aerod*., **54-55**, 657-669.

Ding, F. (2013), "Optimization-based approach for wind tunnel derived load combinations of tall buildings", MPhil Thesis, Hong Kong University of Science and Technology.

Fenn, R. (2001), *Geometry*, London: Springer.

Holmes J.D. (2002), "Effective static load distributions in wind engineering", *J. Wind Eng. Ind. Aerod.*, **90**(2), 91-109. https://doi.org/10.1016/S0167-6105(01)00164-7.

Huang, M.F., Tu Z., Li Q., Lou W.J. and Li Q.S. (2017), "Dynamic wind load combination for a tall building based on copula functions", *Int. J. Struct. Stab. Dyn.*, **17**(8), 298-321. https://doi.org/10.1142/S0219455417500924.

Isyumov, N. (1982), "The aeroelastic modeling of tall buildings", (Ed., Reinhold, T.A.), *Wind Tunnel Modeling for Civil Engineering Applications*, 373-407.

Isyumov, N., Ho, E. and Case, P. (2014), "Influence of wind directionality on wind loads and responses", *J. Wind Eng. Ind. Aerod.*, **133**, 169-180. https://doi.org/10.1016/j.jweia.2014.06.006.

Kareem, A. and Zhou, Y. (2003), "Gust loading factor-past, present and future", *J. Wind Eng. Ind. Aerod.*, **91**(12-15), 1301-1328. https://doi.org/10.1016/j.jweia.2003.09.003.

Kasperski, M. (1992), "Extreme wind load distributions for linear and nonlinear design", *Eng. Struct.*, **14**(1), 27-34. https://doi.org/10.1016/0141-0296(92)90005-B.

Kim Y.C, Tamura Y. and Kim S. (2016), "Wind load combinations of atypical supertall buildings", *J. Struct. Eng.*, **142**(1), 04015103. https://doi.org/10.1061/(ASCE)ST.1943-541X.0001359.

Lin, Y. (1976), *Probabilistic Theory of Structural Dynamics*, Huntington, N.Y: R.E. Krieger Pub. Co.

Makino, A. and Mataki, Y. (1993), "Combination method of maximum response in consideration of statistical correlation of wind forces acting on high-rise building: study on rectangular section models", (Ed., Cook N.J.), *Wind Engineering: 1st IAWE European and African Regional Conference*, 257-266.

Naess, A., Gaidai, O. and Batsevych, O. (2009), "Extreme value statistics of combined load effect processes", *Struct. Saf.*, **31**(4), 298-305. https://doi.org/10.1016/j.strusafe.2008.09.004.

Reinhold, T.A. (1982), "Wind tunnel modeling for civil engineering applications", *Proceedings of the International Workshop on Wind Tunnel Modeling Criteria and Techniques in Civil Engineering Applications*, Gaithersburg, Maryland, U.S.A.

Stathopoulos, T., Elsharawy, M. and Galal, K. (2013), "Wind load combinations including torsion for rectangular medium-rise buildings", *Int. J. High-Rise Build.*, **2**(3), 245-255.

Tamura, Y., Kawai, H., Uematsu, Y., Kondo, K. and Ohkuma, T. (2003a), "Revision of AIJ Recommendations for wind loads on buildings", *Proceedings of the International Wind Engineering Symposium*, Tamsui, Taipei County, Taiwan.

Tamura, Y., Kikuchi, H. and Hibi, K. (2003b), "Quasi-static wind load combinations for low- and middle-rise buildings", *J. Wind Eng. Ind. Aerod.*, **91**(12-15), 1613-1625. https://doi.org/10.1016/j.jweia.2003.09.020.

Tamura, Y., Kikuchi, H. and Hibi, K. (2008), "Peak normal stresses and effects of wind direction on wind load combinations for medium-rise buildings", *J. Wind Eng. Ind. Aerod.*, **96**(6-7), 1043-1057. https://doi.org/10.1016/j.jweia.2007.06.027.

Tschanz, T., Davenport, A. (1983), "The base balance technique for the determination of dynamic wind loads", *J. Wind Eng. Ind. Aerod.*, **13**(1-3), 429-439. https://doi.org/10.1016/0167-6105(83)90162-9.

University of Western Ontario: Boundary Layer Wind Tunnel Laboratory (2007), *Wind Tunnel Testing, A General Outline*, Ontario, Canada.

Xie, J., Irwin, P. and Accardo, M. (1999), "Wind load combinations for structural design of tall buildings", *Wind engineering into the 21st century: Proceedings of the 10th International Conference on Wind Engineering*, Copenhagen, Denmark.

Zhou, Y., Gu, M. and Xiang, H.F. (1999), "Alongwind static equivalent wind loads and response of tall buildings. Part I: Unfavorable distributions of static equivalent wind loads", *J. Wind Eng. Ind. Aerod.*, **79**(1-2), 135-150. https://doi.org/10.1016/S0167-6105(97)00297-3.

Zhou, Y., Kijewski, T. and Kareem, A. (2003), "Aerodynamic loads on tall buildings: An interactive database", *J. Struct. Eng. - ASCE*, **129**(3), 394-404. https://doi.org/10.1061/(ASCE)0733-9445(2003)129:3(394).

AD